Applied and Environmental Microbiology, Sept. 2011, p. 5945–5954 Vol. 77, No. 17
0099-2240/11/$12.00 doi:10.1128/AEM.03022-10

Novel Virulent and Broad-Host-Range *Erwinia amylovora* Bacteriophages Reveal a High Degree of Mosaicism and a Relationship to *Enterobacteriaceae* Phages▽†

Yannick Born,[1,2] Lars Fieseler,[2]* Janine Marazzi,[2] Rudi Lurz,[3] Brion Duffy,[1] and Martin J. Loessner[2]

Agroscope Changins-Wädenswil ACW, Swiss National Competence Center for Fire Blight, 8820 Wädenswil, Switzerland[1]; Institute of Food, Nutrition, and Health, ETH Zürich, 8092 Zürich, Switzerland[2]; and Max Planck Institute for Molecular Genetics, 14195 Berlin, Germany[3]

Received 24 December 2010/Accepted 5 July 2011

A diverse set of 24 novel phages infecting the fire blight pathogen *Erwinia amylovora* was isolated from fruit production environments in Switzerland. Based on initial screening, four phages (L1, M7, S6, and Y2) with broad host ranges were selected for detailed characterization and genome sequencing. Phage L1 is a member of the *Podoviridae*, with a 39.3-kbp genome featuring invariable genome ends with direct terminal repeats. Phage S6, another podovirus, was also found to possess direct terminal repeats but has a larger genome (74.7 kbp), and the virus particle exhibits a complex tail fiber structure. Phages M7 and Y2 both belong to the *Myoviridae* family and feature long, contractile tails and genomes of 84.7 kbp (M7) and 56.6 kbp (Y2), respectively, with direct terminal repeats. The architecture of all four phage genomes is typical for tailed phages, i.e., organized into function-specific gene clusters. All four phages completely lack genes or functions associated with lysogeny control, which correlates well with their broad host ranges and indicates strictly lytic (virulent) lifestyles without the possibility for host lysogenization. Comparative genomics revealed that M7 is similar to *E. amylovora* virus ΦEa21-4, whereas L1, S6, and Y2 are unrelated to any other *E. amylovora* phage. Instead, they feature similarities to enterobacterial viruses T7, N4, and ΦEcoM-GJ1. In a series of laboratory experiments, we provide proof of concept that specific two-phage cocktails offer the potential for biocontrol of the pathogen.

Fire blight is a devastating plant disease caused by the Gram-negative bacterium *Erwinia amylovora*. The disease affects species of the *Rosaceae* family, mainly plants belonging to the pome fruit subfamily *Maloideae*, e.g., apple, pear, and quince (39, 56). After infection (e.g., through the nectarthodes or small lesions), bacterial multiplication leads to the collapse of the parenchyma and to the migration of the bacteria into the plant tissue, causing the typical symptoms of fire blight: necrosis, wilting, and ooze production (58). Depending upon the climatic conditions during the flowering period, fire blight outbreaks can destroy entire trees and orchards within a single season. Since its first observation in the 1780s, fire blight has spread within North America, Central Europe, the Middle East, and New Zealand. In affected countries, it is the major threat to sustainable pome fruit production, resulting in severe economic losses (8) through reduced yield, trade barriers, tree and orchard decimation, sanitation labor, and eradication regulations (16). Since the late 1950s until today, the primary and most reliable control option against fire blight is the application of antibiotics (e.g., streptomycin, oxytetracycline, and gentamicin). However, antibiotic use involves practical drawbacks in terms of pathogen resistance development (28) and regulatory restrictions based upon public health risks (46). Therefore, alternatives, like biological control methods, are in urgent demand from conventional, integrated, and organic growers (26, 27).

Biological control with bacteriophages (phages) features several advantages. Phages are considered natural and ubiquitously distributed, and they represent the most abundant group of biological entities in our environment (9). Their isolation, production, and storage are relatively simple and inexpensive. In general, phages infect only a specific host group, leaving other resident bacteria unharmed. The strictly virulent, nontransducing phages are regarded as environmentally safe tools for the control of bacterial pathogens (22). The potential of phages for the biocontrol of *E. amylovora* and other plant pathogens (e.g., *Pectobacterium carotovora*, *Xanthomonas campestris* pv. vesicatoria, and *Agrobacterium tumefaciens*) has been demonstrated (4, 6, 20, 21, 45, 49, 53). Balogh et al. (5) offer a thorough review of the history, success, and unique considerations for phage therapy in plant agriculture.

The first *E. amylovora* phages were described in the 1970s (18, 47). Later on, several *E. amylovora*-infecting phages were isolated and classified into different subtypes based on plaque morphology, host range analysis, electron microscopy, restriction fragment length polymorphism (RFLP), and PCR (21, 50). The current sequence information is limited, as the genome sequences of phages of only two types are available: the podovirus ERA103 (NC_009014) and its relatives ΦEa1h and

* Corresponding author. Mailing address: Institute of Food, Nutrition, and Health, ETH Zürich, Schmelzbergstrasse 7, CH-8092 Zürich, Switzerland. Phone: (41) 44 632 33 34. Fax: (41) 44 632 12 66. E-mail: lars.fieseler@ilw.agrl.ethz.ch.

† Supplemental material for this article may be found at http://aem.asm.org/.

▽ Published ahead of print on 15 July 2011.

ΦEa100 (40) and the Felix O1-like myovirus ΦEa21-4 (35) and its close relative ΦEa104 (40).

Major challenges in phage therapy for plant disease control are the emergence of resistant strains and environmental factors that would rapidly reduce the number of infective phages, particularly desiccation and UV destruction (5). The phage persistence in the phyllosphere can be improved by appropriate formulations (6) and by avoiding exposure to sunlight. The probability of the development of phage-resistant strains can be reduced by the application of cocktails consisting of phages featuring different replication pathways. Therefore, a thorough characterization of the phages, including sequencing of the complete genomes, is required if they are intended to be used as biocontrol agents.

We report here the isolation of a set of *E. amylovora*-infecting phages and the complete sequencing and molecular analysis of the phages L1, M7, S6, and Y2. Moreover, we demonstrate that specific two-phage cocktails are well suited to control *E. amylovora in vitro*. The data presented yield novel insights regarding the molecular biology of *E. amylovora* phages and provide a sound basis for their development as fire blight biocontrol agents.

MATERIALS AND METHODS

Bacterial strains and culture conditions. Strains of *Erwinia* spp. and *Pantoea* spp. were grown in Luria Bertani (LB) broth at 30°C or at 27°C when grown on plates. *Escherichia coli* strain XL1-Blue MRF′ (Agilent Technologies, Santa Clara, CA) was cultivated in LB at 37°C.

Phage isolation and propagation. Soil samples were collected from 32 locations throughout Switzerland between the years 2007 and 2009. Locations that had orchard and old-growth landscape apple or pear trees and that had a recorded recent, a historical, or no fire blight outbreak were chosen. Phages were isolated and enriched by a standard method. Briefly, 190 ml of SM-buffered (50 mM Tris, 100 mM NaCl, 8 mM $MgSO_4$, pH 7.4) LB broth was inoculated with 10 ml of an overnight culture of one of several different *E. amylovora* host strains. The use of various bacterial strains increases the probability of the isolation of diverse phage types (21). Ten grams of soil was added and incubated under constant agitation at 30°C. After 18 h, soil and bacterial host cells were pelletized by centrifugation (1 min, 10,000 × *g*), and the supernatant was filtered (0.2-μm-pore-size filter; Sarstedt, Nümbrecht, Germany). Phage presence was determined using the soft-agar overlay method (2) by spotting 10 μl of the supernatant onto LB+ soft agar (LB containing 1% [wt/vol] glucose, 2 mM $MgSO_4$, and 0.4% [wt/vol] agar) inoculated with freshly growing *E. amylovora*. Phages were isolated by picking individual plaques using a Pasteur pipette and resuspended in 250 μl SM buffer. This step was repeated at least twice to ensure the purity of the phage isolate. To propagate each phage, 40 soft-agar overlay plates with semiconfluent phage lysis were produced. Phages were recovered from the plates by the addition of SM buffer to the top surface (5 ml per plate). Then, the plates were gently agitated at room temperature (RT) (20 rpm, 6 h; Heidolph Polymax 1040), and the buffer liquid was harvested. Phages were precipitated using polyethylene glycol (10% [wt/vol] PEG 8000, 1 M NaCl; 4°C, overnight) and pelletized (10 min, 10,000 × *g*), and the pellet was resuspended in 5 ml SM buffer. Phages were purified using CsCl gradient centrifugation (48) for subsequent electron microscopic analysis and DNA extraction.

Phage nomenclature. For the submission of the genome sequences to GenBank, we named the phages according to the current bacterial virus nomenclature to ensure a clear identification (e.g., L1 is vB_EamP-L1, with vB as the virus of bacteria; Eam as *E. amylovora*, the host species; P as *Podoviridae*, the virus family; followed by L1, the laboratory name) (33). For reasons of simplicity, only the laboratory names are used in this paper.

Host range analysis. Using the soft-agar overlay method (2), all phage isolates were tested for their abilities to infect a collection of *E. amylovora* strains and closely related species. The occurrence of single plaques in the soft-agar overlay was determined after overnight incubation at 27°C.

Phage DNA extraction and analysis. CsCl-purified virus particles were dialyzed against a 1,000-fold excess of SM buffer (6 h, RT) and afterwards treated for 1 h at 56°C with EDTA (pH 8.0, 20 mM), proteinase K (50 μg/ml), and SDS (0.5% [wt/vol]). DNA was isolated and purified using a phenol-chloroform extraction procedure as described previously (32, 48). The phage whole-genome sizes were determined by pulsed-field gel electrophoresis (PFGE) as described earlier (30) using a Chef DR III apparatus (Bio-Rad, Reinach, Switzerland).

TEM. For transmission electron microscopy (TEM) imaging, CsCl-purified phages were negatively stained with 2% (wt/vol) uranyl acetate, 2% (wt/vol) ammonium molybdate, or 2% (wt/vol) Na-phosphotungstic acid and then analyzed as previously described (32). Actual magnifications were determined using cross grating replica or catalase crystals (Electron Microscopy Sciences, Hatfield, PA) (60).

Genome sequencing and bioinformatic analysis. The genomes of L1, S6, and Y2 were sequenced using a shotgun approach. Genomic libraries of L1 were constructed by cloning TasI- and MspI-digested DNA into EcoRI- and ClaI-linearized cloning vector pBluescript II SK(−) (Agilent Technologies), respectively. A third library was generated by sonication. DNA was sheared, followed by gel extraction of fragments of 1.0 to 2.5 kbp in size. The fragments were end repaired (End-It DNA end repair kit; Epicentre Biotechnologies, Madison, WI) and inserted into EcoRV-linearized pBluescript II SK(−). The libraries of S6 and Y2 genomic DNA were generated after sonication only. The vectors were electroporated (2.5 kV, 25 μF, 200 Ω; GenePulser; Bio-Rad, Hercules, CA) into electrocompetent *E. coli* XL1-Blue MRF′ cells and incubated on LB plates containing ampicillin (100 μg/ml) and tetracycline (10 μg/ml) at 37°C. The addition of 80 μg/ml X-Gal (5-bromo-4-chloro-3-indolyl-β-D-galactopyranoside) and 20 mM IPTG (isopropyl-β-D-1-thiogalactopyranoside) to the plates enabled the identification of insert-bearing clones by blue/white screening. Constructs containing inserts of 1.0 to 2.5 kbp in size were selected for sequencing using the ABI 3730xl DNA analyzer (Sanger Technology). Sequences were assembled using the ContigExpress module of Vector NTI Advance 10 (Invitrogen, Paisley, United Kingdom) with default parameters and CLC Main Workbench 5 (CLC Bio, Aarhus, Denmark). Gaps were closed by primer walking using phage DNA as the template. Every position was sequenced at least twice. Phage M7 was sequenced using the Roche GS FLX system with Titanium reagents and the Roche GS Assembler 2.3 software (default settings) for sequence assembly.

Open reading frames (ORFs) of all phage genomes were predicted using CLC Main Workbench 5 and Vector NTI software; the minimal ORF length was set to 30 codons, with ATG, GTG, or TTG as start codons and TAA, TGA, or TAG as stop codons. Putative genes were annotated based on similarities to database entries and the presence of a putative Shine-Dalgarno sequence (ribosome binding site) similar to the consensus sequence of *E. coli* GGA GGT (51). Translated amino acid sequences were then compared to the nonredundant GenBank protein database, using BlastP (3). Pairwise alignments were performed with CLC Main Workbench 5.

Peptide mass fingerprinting. Structural proteins were separated by horizontal SDS-PAGE as outlined previously (15). Distinct bands were excised from the gels, and the polypeptides were analyzed using liquid chromatography/tandem mass spectrometry (LC/MS-MS) as described earlier (32, 62). The identified proteins were compared to all possible ORFs >60 nucleotides (nt) in size and summarized using Scaffold 2 Proteome Software (Proteome Software Inc., Portland, OR).

Determination of genome end structures. Physical structures of the genome ends were determined as described elsewhere (32, 37). Briefly, phage DNA was treated with BAL31 nuclease (NEB, Ipswich, MA) at 30°C for different incubation times prior to digestions with selected restriction enzymes. For the identification of potential cohesive ends (*cos*), half of the restriction-digested phage DNA was incubated at 62°C for 10 min to separate potentially ligated *cos* sites and immediately stored on ice. The RFLP patterns were then analyzed for changes. Based on RFLP and BAL31 experiments, the genome ends could roughly be localized. Primers were designed that annealed approximately 300 bp apart from the expected ends to initiate sequencing toward the putative ends. An abrupt drop-off in the sequencing signal intensity indicated the physical end of the phage genomic DNA molecule. The experimental data were verified by phylogenetic analysis of the large terminase proteins (11). A tree was constructed by applying the neighbor-joining method (1,000 bootstrap replicates) using alignments generated with the following parameters: gap open cost, 10; gap extension cost, 1; end gap cost, free (CLC Main Workbench 5).

***In vitro* activity.** The efficacies of the strictly virulent phages L1, M7, S6, and Y2 to control *E. amylovora* were tested *in vitro*. Strain CFBP 1430 (10^5 CFU/ml) was infected with 10^8 PFU/ml in 4 ml LB broth. The efficacies of two-phage cocktails were determined by mixing equal amounts of individual phages to reach a total concentration of 10^8 PFU/ml (i.e., 5×10^7 PFU/ml of each phage). The phage-bacterium mixtures were incubated at 30°C under constant shaking. Suspensions of bacteria and phage were dilution plated immediately after phage addition (0 h) and after 1, 2, 4, 6, 8, and 24 h of incubation to determine the CFU/ml of

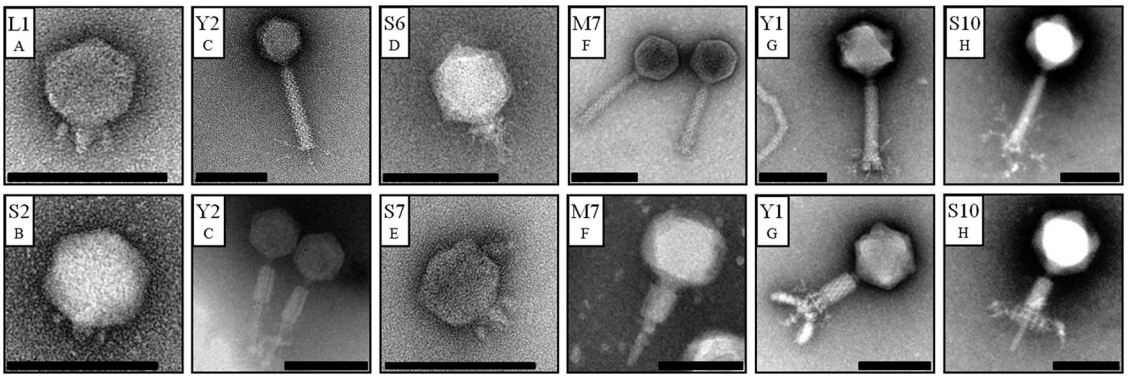

FIG. 1. Electron micrographs of negatively stained *Erwinia amylovora* phages. Phages were classified into the *Podoviridae* (L1, S2, S6, and S7) and *Myoviridae* (Y2, M7, Y1, and S10) families. From the latter, virions with both contracted and uncontracted tails are shown. Letters A to H indicate phage subtypes. Scale bars represent 100 nm.

surviving bacteria. The plates were incubated at 27°C until quantification of viable bacteria. Each experiment consisted of three replicates per treatment and was carried out at least three times.

Nucleotide sequence accession numbers. Complete nucleotide sequences of L1 (HQ728265), M7 (HQ728263), S6 (HQ728266), and Y2 (HQ728264) were deposited in GenBank under the accession numbers listed in parentheses.

RESULTS

Novel *E. amylovora* phages feature unique characteristics. Preliminary results from plaque morphology, PFGE, RFLP, and host range analysis indicated that the 24 phage isolates can be grouped into eight subtypes (A to H). From each type, a single representative was selected for further examination by electron microscopy. They belong to the *Myoviridae* or *Podoviridae* family, having either A1 or C1 morphotypes, respectively (1). Their capsid diameters range from 58 to 95 nm (Fig. 1). PFGE indicated phage genomes of 39 to 180 kbp in size (Fig. 2). Most phages isolated in this study are novel representatives of phages infecting *E. amylovora* and feature unique characteristics. Only two subgroups are related to the previously described North American isolates (18, 21, 47, 50). Group F phages seem to be similar to group 1 viruses described by Gill et al. (21). This could later be confirmed by sequencing of phage M7 (see below). Basic characterization of group B phages indicated that they resemble phage ΦEa1 (group 3) (21, 47, 50).

Broad host range is a common feature of *E. amylovora* phages. Most phages investigated here were able to infect a majority of tested hosts (Table 1). Phages Y2 and M7 successfully infected all *E. amylovora* strains. Phage Y2 was highly specific toward *E. amylovora*, while other phages also lysed closely related bacteria such as *Pantoea agglomerans* or *Erwinia billingiae* (Table 1).

Genome analyses indicated relatedness to *Enterobacteriaceae* phages. Four broad-host-range phages (L1, S6, Y2, and M7) were chosen for complete genome sequencing. L1 formed distinct plaques surrounded by secondary haloes in soft-agar overlays, suggesting a diffusible enzyme activity. Y2 was selected because of its species specificity, M7 because it infected every *E. amylovora* strain as well as strains of closely related species, and S6 because of its different morphological properties.

The average sequence coverages of the genomes were 4.8-fold (L1), 3.3-fold (S6), 4.7-fold (Y2), and 130-fold (M7). The assemblies of the phage genomes from individual reads yielded unique unit genomes for all four phages. *In silico* predictions were confirmed by restriction enzyme analysis. Table 2 summarizes the major characteristics for the phages sequenced in this study, including data for ΦEa21-4 and ERA103. Additional information on features and database matches of predicted proteins encoded by L1, M7, S6, and Y2 can be found in the supplemental material.

The genome of phage L1 has a length of 39,282 bp with direct terminal repeats of 172 bp. Forty-nine putative open reading frames were annotated based on similarities to proteins in the database as well as on the presence of a potential ribosome binding site preceding the start codon. The putative functions of the gene products (gp) could be grouped into early

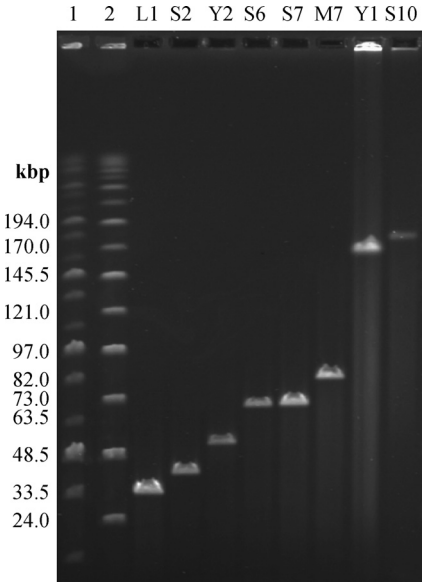

FIG. 2. Pulsed-field gel electrophoresis analysis of full-length *Erwinia amylovora* phage genomes (as indicated). Lanes 1 and 2 include MidRange PFGE markers I and II (NEB), respectively. Sizes are as indicated.

TABLE 1. Host ranges of eight *Erwinia amylovora* phages isolated on different hosts

Species	Host strain	Infectivity of phage (phage group)[a]:							
		L1 (A)	S2 (B)	Y2 (C)	S6 (D)	S7 (E)	M7 (F)	Y1 (G)	S10 (H)
E. amylovora	CFBP1430	+*	+*	+	+	+	+	−	+*
	CFBP1232	+	+	+	+	+	+	−	+
	Ea153	+	+	+	+	+	+	−	+
	Ea1/74	+	+	+	+	+	+	−	+
	Ea1/79	+	+	+	+	+	+	−	+
	ACW38899	+	+	+	+	+	+	−	+
	ACW56400	+	+	+	+*	+*	+	+	+
	ACW44274	+	+	+	+	+	+	−	+
	ACW42912	+	+	+	+	+	+	−	+
	ACW30560	+	+	+	+	+	+	−	+
	Ea Rac 3075	+	+	+	+	+	+	−	+
	ACW55500	+	+	+	+	+	+	−	+
	ACW55835	+	+	+	+	+	+	−	−
	ACW55955	+	+	+	+	+	+	−	+
	Ea4/82	−	−	+*	+	+	+	−	−
	IPV 1077/7	+	+	+	+	+	+	+	+
	IPV-BD 5357	+	+	+	+	+	+	+*	+
	01SFR-BO	+	−	+	+	+	+	−	−
	OMPBO 691.2	+	+	+	+	+	+	+	−
	LA 469	−	+	+	+	+	+	−	−
	LA 071	−	−	+	+	+	+	−	−
	LA 411	+	+	+	+	+	+	−	+
	LA 468	+	+	+	+	+	+	−	−
	LA 477	−	−	+	−	−	+*	−	−
Erwinia persicina	ACW40943	−	−	−	−	−	+	−	−
	ACW40560x	−	−	−	−	−	−	−	−
	ACW41072	−	−	−	−	−	−	−	−
Erwinia billingiae	B90	−	−	−	−	+	+	−	−
Pantoea agglomerans	Eh 42	−	−	−	−	−	+	−	−
	Em 406	−	−	−	−	+	−	−	−
	Em 283	+	+	−	−	+	−	−	−
Pantoea vagans	C9-1	−	−	−	−	+	−	−	−
Pantoea ananatis	351 Lys	+	+	−	−	+	−	−	+

[a] +, sensitive; −, no infection. Isolation strains are highlighted with asterisks. Phage groups are given in parentheses.

and late gene clusters (Fig. 3). The early gene cluster comprises genes that are involved at the beginning of the infection process in host takeover, DNA replication, modification, and translation. The late gene cluster is composed of structural, DNA assembly, and cell lysis proteins. The lack of a lysogeny control region indicates that it also is a virulent phage. L1 is a member of the T7-like phages: the genomes of L1 and T7 share a 61.2% nucleotide identity over their full lengths and feature the same architectures, with function-specific clusters and transcription exclusively from left to right. Out of 49 putative gene

TABLE 2. Major characteristics of *Erwinia amylovora* phages

Characteristic	L1	S6	Y2	M7	ΦEa21-4	ERA103
Virus family[a]	C	C	A	A	A	C
Lifestyle	Virulent	Virulent	Virulent	Virulent	Virulent	Virulent
Capsid diameter (nm)	58	66	67	77	60	ND[c]
Tail length (nm)			124	116	90	
Genome size (kbp)	39.3	74.7	56.6	84.7	84.6	45.4
Genome structure[b]	DTR	DTR	DTR	DTR	DTR	DTR
G+C content (mol%)	51.9	52.1	44.2	43.4	43.8	49.8
No. of predicted ORFs/no. of ORFs with function assigned	49/27	115/18	90/14	117/30	117/23	53/29
Reference	This study	This study	This study	This study	35	NC_009014

[a] A, *Myoviridae*; C, *Podoviridae* (according to Ackermann [1]).
[b] DTR, direct terminal repeats.
[c] ND, not determined.

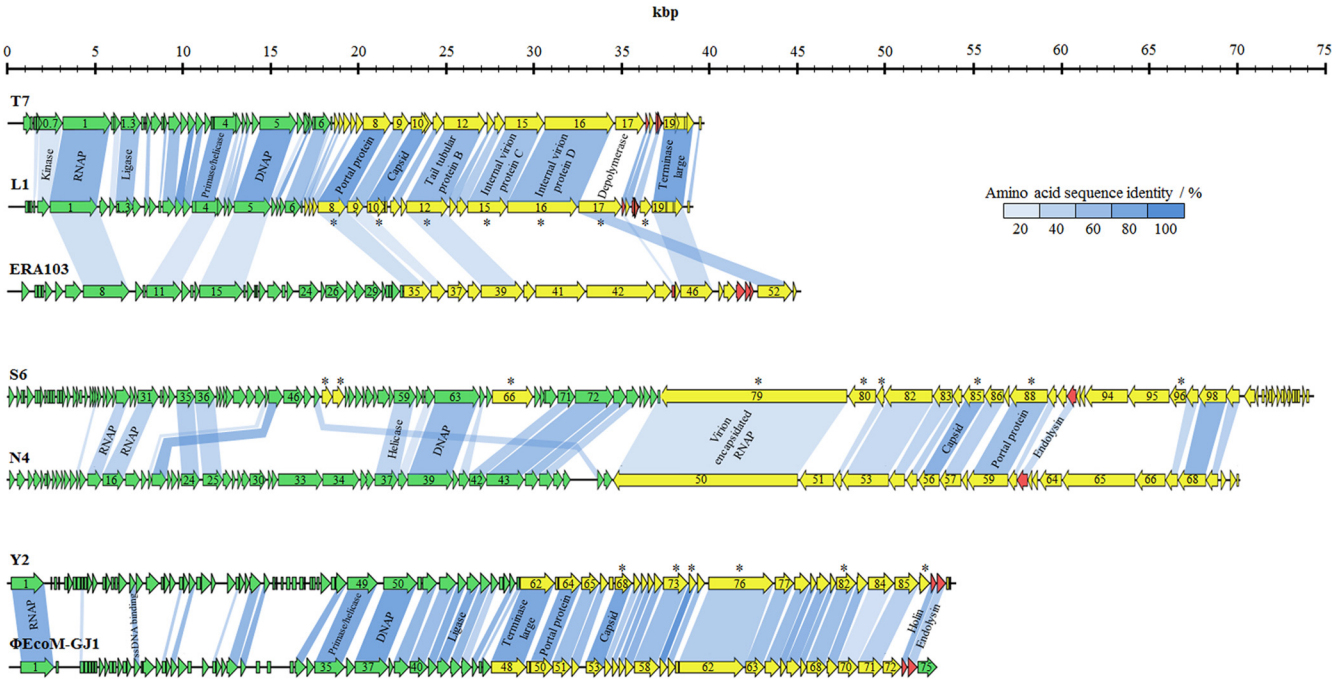

FIG. 3. Genome maps of phages L1, S6, and Y2 and alignment with related phages. Genes were classified into functional clusters based on database comparisons, peptide fingerprinting, and their locations on the genome. They are represented in green (early genes), yellow (late genes), and red (lysis genes). Shading indicates the degree of amino acid sequence identity of gene products with an identity of >20%. Putative functions of selected genes are indicated. Gene products that were identified using mass spectrometry are marked with an asterisk.

products, 24 share overall sequence identities of more than 50% with T7 proteins (17). Only 10 gene products have identities below 20% (Fig. 3). Further common features are the putative internal in-frame start in *orf04* (primase/helicase) at nucleotide position 10676 of L1 producing gp4B (helicase domain) and a potential frameshift in the gene encoding the major capsid protein of L1 (gp10A). A putative frameshift site was identified at nucleotide positions 21483 to 21488 (GUU UUC), where the phenylalanine-tRNA can also pair in the −1 frame. The stop codon of the −1 frame is located 145 nt downstream of the frameshift site and extends gp10A by an additional 43 amino acids, generating the minor capsid protein (gp10B). In T7, the frameshift also consists of overlapping phenylalanine codons (13, 38). A potential transcriptional terminator is located approximately 200 nt downstream of the frameshift site in both phages.

Phage S6 has a genome size of 74,669 bp, including direct terminal repeats of 397 bp. A function was assigned to 18 out of 115 putative gene products (Table 2). In contrast to phage L1, the early and late genes are oriented in opposite directions (Fig. 3). The first gene in the late gene cluster encodes a putative virion-encapsidated RNA polymerase (vRNAP). This genome organization resembles those of *E. coli* phage N4 (19, 29) and other N4-like phages infecting marine roseobacters (DSS3Φ2, EE36Φ1) (61) and *Pseudomonas aeruginosa* (LUZ7, LIT1, PEV2) (12). A major hallmark of N4-like phages is the use of three different DNA-dependent RNA polymerases during their growth cycles (29). Unlike other phages, N4 uses the vRNAP for the transcription of the early genes. The vRNAP is functionally present in the capsid and injected into the host cell during infection (19, 29). Phages S6 and N4 display significant similarities across their entire genomes, sharing an overall nucleotide sequence identity of 54.4%, with 29 gene products having greater than 20% sequence identity (Fig. 3). However, putative functions could not be assigned to each of them.

Phage Y2 features a 56,621-bp genome with invariable genome ends and long direct terminal repeats of 2,608 bp. Ninety ORFs were annotated (Table 2). Similarly to L1 and S6, phage Y2 is strictly virulent since it does not possess a lysogeny control region (Fig. 3). Transcription of the ORFs is exclusively from left to right. Gene products involved in host takeover and DNA metabolism are located at the left end of the genome in the early gene cluster. The late gene cluster and the cell lysis cassette are located at the right end. Y2 shows high sequence identities only to ΦEcoM-GJ1, a phage infecting porcine enterotoxigenic *E. coli* strains (25). They share a 61.0% overall nucleotide sequence identity and 43 gene products with sequence identities above 20%.

Sequencing of phage M7 yielded an 84,694-bp genome, with direct terminal repeats of 444 bp. A putative function of the 117 annotated ORFs was found for 30 gene products (Table 2). The densely distributed ORFs are interrupted by an ~3.5-kbp region, including a series of tRNAs. No lysogeny control region was identified, confirming the strictly lytic life cycle of M7. Comparative genomics revealed its close relationship to the Felix O1-like phage ΦEa21-4 (35). The overall nucleotide sequence identity between these two phages is 87.4%, and their genome architectures are virtually identical. Thus, M7 was considered a close relative of ΦEa21-4 and was not studied further (except for its genome structure [see below]).

Proteomes of *E. amylovora* phages. Peptide mass fingerprinting identified eight structural proteins of L1, nine of S6, and six

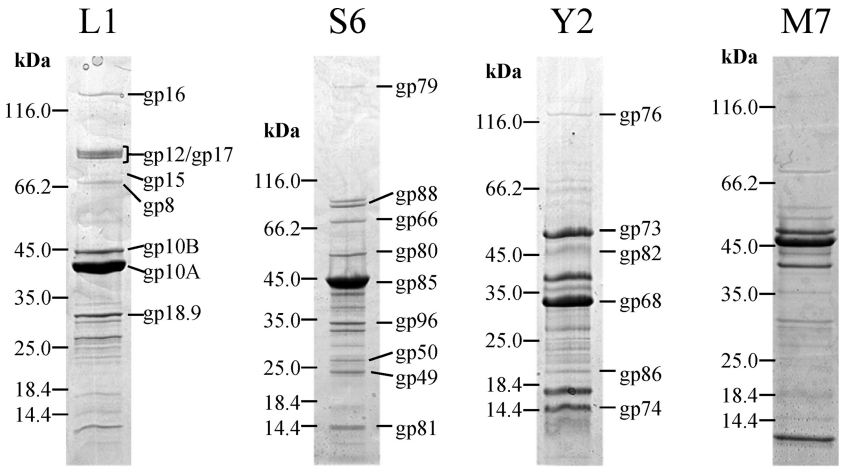

FIG. 4. Analysis of virion proteins of phages L1, S6, Y2, and M7 by SDS-PAGE. Molecular mass markers are indicated on the left of each gel segment. Identification of individual protein bands was performed by peptide fingerprinting and mass spectrometry. The corresponding gene product names are indicated on the right (except for phage M7).

of Y2 (M7 was not analyzed); corresponding genes are marked with asterisks in Fig. 3. Putative capsid components are the most prominent bands on the SDS gels (Fig. 4). The minor capsid protein of L1 (gp10B) was identified on the gel with a molecular mass approximately 5 kDa greater than that of the major capsid protein gp10A. Both gp10A and gp10B were found to be encoded by the same gene. This confirms the frameshift at nucleotide positions 21483 to 21488 (see above). The differing intensities of the protein bands allowed for an estimated quantification of the number of frameshift events. The band of gp10A is roughly 10-fold more intense than the band of gp10B, indicating that the frameshift occurs in 10% of the recoding events. This is similar to T7 (13). Other proteins of L1 identified as structural components are the putative portal protein (gp8), the tail tubular protein B (gp12), internal virion proteins C and D (gp15, gp16), an exopolysaccharide (EPS) depolymerase (gp17), and an unknown structural protein (gp18.9).

Phage S6 possesses a component (gp79) which is significantly larger than its other structural proteins. It was identified as the putative vRNAP. A set of three proteins (gp49, gp50, and gp66) encoded in the early gene region (i.e., left of the putative vRNAP gene) was also found to be present in the mature virion. Unfortunately, functional predictions could not be made, as there were no closely related proteins in the database. Other structural proteins of S6 are the major capsid protein (gp85), the portal protein (gp88), and three unknown proteins (gp80, gp81, and gp96).

As phage Y2 is relatively novel, there is very limited information available on similar phages. Besides the major capsid protein (gp68), a putative tail fiber (gp76) was identified. The functions of other structural components, such as gp73, gp74, gp82, and gp86, are unknown.

Phage genomes L1, M7, S6, and Y2 feature direct terminal repeats of different lengths. Our data showed that all four phages contain invariable genome ends. Restriction digestion analysis after BAL31 nuclease treatment of phage DNAs revealed that the two fragments located at the distal portions of the phage DNA molecules were progressively shortened by the enzyme, until they completely disappeared (Fig. 5). In some cases (e.g., AsnI- or FspBI-treated S6-DNA), the disappearing fragments were not visible because of their relatively small sizes (<1,000 nt). In the case of terminally redundant, circular permuted genomes, all fragments would have been degraded simultaneously by BAL31 (37). The phage genomes also lack cohesive ends, since heat treatment prior to electrophoresis did not change the restriction patterns (10) (data not shown). To confirm the genome end structures, sequencing primers were designed that bind in a suitable distance to the putative ends to initiate synthesis toward the physical end of the genome. When linear phage DNA or isolated terminal fragments were used as templates, typical sudden drop-offs of the Sanger sequencing signals were observed. It was found that the sequences of the two individual ends of phages L1, M7, S6, and Y2 feature direct terminal repeats of 172 bp, 444 bp, 397 bp, and 2,608 bp, respectively. Phylogenetic analysis of the large terminase proteins confirmed the experimental data for phages L1, M7, and S6. The terminases cluster together with terminases of phages having similar packaging strategies (Fig. 6). The Y2 terminase was found to be similar to terminases of phages with a T1-like headful packaging mechanism.

Phage cocktails efficiently control *E. amylovora*. The application of a single virulent phage did not result in a complete eradication of *E. amylovora*. However, specific combinations of two different phages (L1/Y2 and L1/S6) very efficiently reduced the viable counts below the detection limit (50 CFU/ml) after 1 h of incubation (Fig. 7). Other phage combinations had no enhanced efficacy compared to that of the single phages (e.g., M7/S6 and others; data not shown). After 24 h, all bacterial cultures exposed to phage showed regrowth. Nevertheless, the remaining cell counts were significantly reduced in all samples compared to that of the uninfected control. Using single phages, reductions of 0.5 (L1), 2.5 (M7), 2.0 (S6), and 2.9 (Y2) logs (CFU/ml) were achieved. Applying two-phage cocktails, final viable counts were reduced by 3.1 (L1/S6), 3.3 (L1/Y2), and 1.6 (M7/S6) logs (CFU/ml). The observed effects could be reproduced using other *E. amylovora* strains (i.e., ACW56400, ACW55500, and LA411).

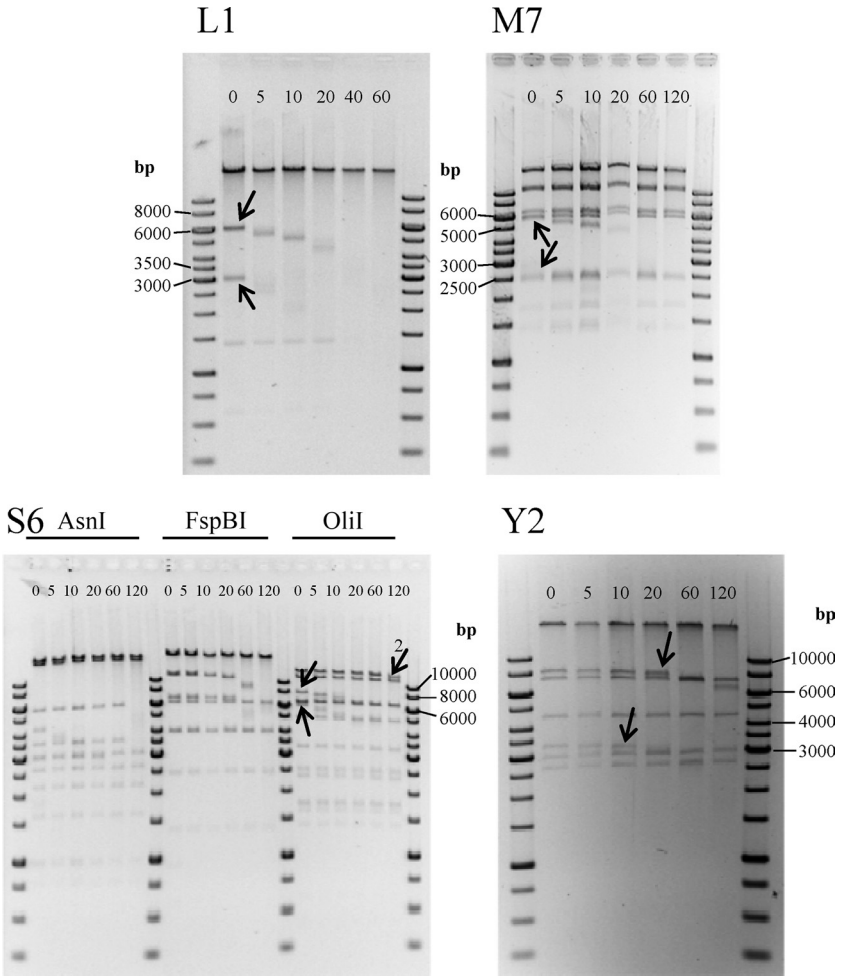

FIG. 5. Analysis of phage genome physical structures. Shown are fragment patterns of phage DNA, following time-limited BAL31 treatment and subsequent digestion with different endonucleases. Phage L1 was digested with MfeI, M7 with FspBI, S6 with three different restriction endonucleases, and Y2 with OliI. Arrows indicate terminal fragments, which are progressively shortened by the BAL31 nuclease. The numbered arrow in the lower left panel (S6) indicates the second-to-last fragment, which is shortened only after the terminal fragment is completely degraded. Incubation times with BAL31 in minutes are indicated at the top of each gel.

DISCUSSION

A set of 24 novel phage isolates infecting *E. amylovora* was isolated. Based on host range, virion morphology, genome size, and DNA restriction patterns, they could be grouped into eight subtypes. Only two subtypes appeared related to previously described phages from samples collected in North America (21). Sequencing of phages L1, M7, S6, and Y2 revealed relationships to phages infecting other members of the *Enterobacteriaceae*. Phages L1, S6, and Y2 are novel among *E. amylovora* phages, with little relatedness to other known phages infecting this species. It is possible that they have evolved more or less recently, during a process of adaptation to *E. amylovora* in the second half of the last century, when the pathogen arrived in Central Europe (8). The close relationship of M7 and the Felix O1-like virus ΦEa21-4 (35) and the relatedness between group B and ΦEa1-like phages (21) could indicate that *E. amylovora* phages also spread from North America to Central Europe. It is unclear if the different phage isolates are just a result of diverse strains used for the isolation or if the phage collections represent the local phage populations. The possible influence of isolation strains on the phage variety was reported earlier (21, 50). Using *E. amylovora* strain Ea110 as a host, a distinct phage similar to ΦEa1 was repeatedly isolated (50). In our study, the variety of phages did not increase proportionally to the total number of phage isolates, and a plateau may have been reached due to the use of a particular set of propagation strains.

The broad host ranges observed for most of the phages suggest obligately lytic life cycles, which is an important consideration regarding application of phages against target bacteria (22). True virulent lifestyles could be confirmed for phages L1, M7, S6, and Y2 through sequencing of their genomes. Nevertheless, some *E. amylovora* strains tested were insensitive to phages L1 and S6. A known factor influencing the sensitivity or resistance of *E. amylovora* to phages is the production of a capsule (7). Our observations support this theory. For example, the L1-like small podoviruses (group A), isolated on strain CFBP 1430, were not able to infect strain 4/82, which produces smaller amounts of EPS.

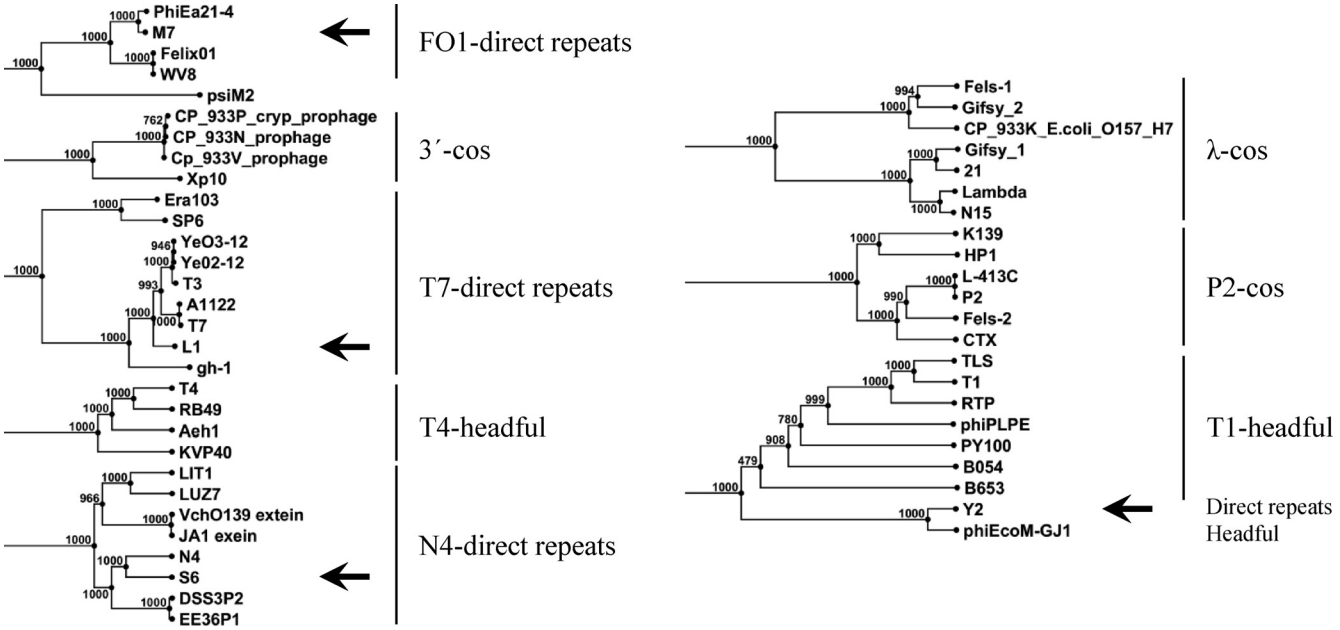

FIG. 6. Phylogenetic analysis of large terminase subunits of phages L1, M7, S6, and Y2 (indicated by arrows) and comparison to other phages with known packaging mechanisms (11, 30) as indicated. The tree was generated from an alignment (gap open cost, 10; gap extension cost, 1; end gap cost, free) using the neighbor-joining method with 1,000 bootstrap replicates (CLC Main Workbench 5).

In addition to a virulent lifestyle and a broad host range, host specificity is of major interest (22). Our analyses showed that several of the 24 phages were able to infect species closely related to *E. amylovora*, which may potentially serve for phage replication in the phyllosphere (5, 34). In contrast, phage Y2 is strictly species specific and therefore unlikely to affect the nonpathogenic resident microflora when applied as a biocontrol agent, even in large quantities.

The inability to transduce nonphage DNA is another desirable property of phages designated for biocontrol purposes. The enterobacterial relatives of the phages described here are not known as generalized transducers (55), which can be explained by their physical genome structures. Their terminase enzymes recognize specific sequence motifs for the internalization of the viral DNA molecules into the newly assembled capsids. This lowers the probability that nonphage DNA is accidentally incorporated into the virus particle (11). Terminases of transducing phages generally feature less stringent sequence specificity. They possess circularly permuted and terminally redundant genomes and package their DNA by a headful mechanism (11). L1, M7, S6, and Y2 feature fixed genome ends and are therefore unlikely to be able to transduce host DNA. Phylogenetic analysis of the large terminase subunits indicated that the L1 terminase is related to terminases of phages T7, T3, and SP6, all of which feature direct terminal repeats of variable lengths (11, 14, 17, 38, 43). Phage S6 clusters together with N4 and other phages that use an N4-like packaging mechanism. Phage N4 has short direct terminal repeats of variable lengths (390 to 440 nt) containing 3′-single-stranded extensions (42). Phylogenetic analysis of the M7 terminase indicated its relatedness to Felix O1-type terminases. Felix O1 and ΦEa21-4 were proposed to have invariable ends with short direct terminal repeats (35, 59), in line with our findings.

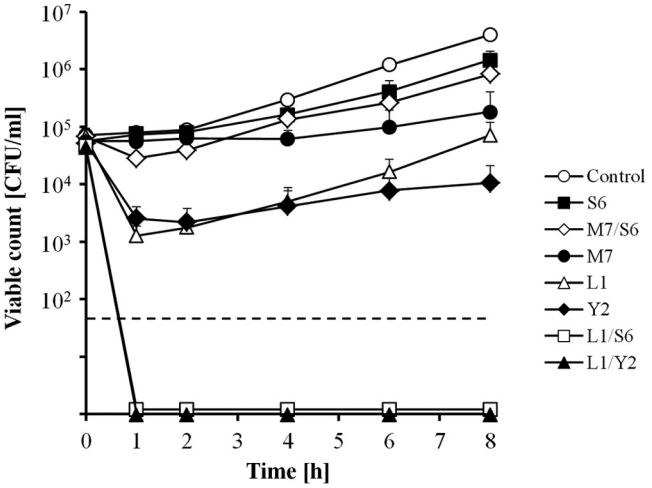

FIG. 7. Viable counts of *E. amylovora* CFBP1430 after infection with single phages or two-phage cocktails. The values indicate the means of results from three independent trials, including standard deviations. The dashed line indicates the detection limit of 50 CFU/ml.

The striking homologies between phages Y2 and ΦEcoM-GJ1 (including their terminases) could suggest a circularly permuted genome for Y2, containing a *pac* site. However, attempts to obtain experimental support for this hypothesis failed, i.e., restriction patterns did not yield the characteristic submolar fragment(s) occurring from digestion of phage DNA molecules originating from *pac*-dependent headful packaging (10). Moreover, BAL31 nuclease simultaneously degraded two fragments, and digestions with various restriction enzymes with n recognition sites always yielded $n + 1$ fragments. Therefore, we

conclude that Y2 does not use headful packaging but that all phage genome molecules are identical and consist of a 54,013-bp information genome and a 3′ terminal repeat of 2,608 bp, yielding a 56,621-bp physical genome.

The clustered organization of the *E. amylovora* phage genomes into transcriptional units is typical for tailed phages, and the architecture is concordant with the model of phage genomes being modular built genetic mosaics (9, 24). This proposed mosaicism likely served as a driving force for the rapid adaptation to new host bacteria. Genetic modules, genes, or entire transcriptional units can be exchanged via a single recombination event. The similarity between two related phages abruptly ceases at the boundaries of genetic material exchanged by horizontal transfer (9). Analogously, L1, M7, S6, and Y2 and their enterobacterial relatives share significant homologies among most late genes, interrupted by gaps with apparently lower sequence identities. These gaps are located mainly in the region encoding tail-associated proteins. In general, host specificity seems to be related to sequence diversities in these tail-associated proteins. In the case of L1, the similarity to T7 is interrupted in gp17, whereas the genome of ERA103 shares stronger similarity to L1 in this particular region. The N-terminal domains of gp17, which link the tail fiber to the tail tube (52), are similar in L1 and T7. The major C-terminal part of L1-gp17 appears to have been replaced by a depolymerase (23, 31, 57), leading to a different function of the tail fiber and, thus, to nonoverlapping host ranges. Genes encoding tail components such as fibers or spikes are known hot spots for recombination. For example, K1-specific *E. coli* phages originating from different ancestors gained their ability to infect encapsulated bacteria via horizontal uptake of an endosialidase gene (54). Although these phages have different ancestors, their host ranges overlap due to the shared tail spikes. Accordingly, the host ranges of L1 and ERA103 overlap due to the presence of tail fibers with a depolymerase activity, even if they likely have different ancestors. Similar observations were made when comparing M7, S6, and Y2 to related enterobacterial phages. The ORFs encoding putative tail structures of M7 (*orf40* to *orf42*) and Felix O1 (*orf77*) are unrelated, while the genes upstream and downstream are homologous. The same findings hold true for S6 and N4. There is an exceptional region of low similarity between S6 and N4 comprising *orf94* and *orf95* of S6. These gene products have putative glycoside hydrolase activity which may facilitate degradation of the host cell capsule during infection, similar to the depolymerase from phage L1. Finally, phage Y2 and ΦEcoM-GJ1 share significant similarities throughout their late gene cluster, with the exception of *orf86* of Y2 and *orf72* of ΦEcoM-GJ1. Again, both regions encode apparently unrelated putative tail fiber components (25).

In vitro experiments indicated a significant reduction of viable host cells by phage infection but also revealed the development of insensitive bacteria following exposure to phage preparations. Earlier studies, including *E. coli*, *Campylobacter jejuni*, and *X. campestris* pv. pruni, also reported the development of temporarily resistant bacteria after phage treatment. It is interesting to note that these resistant bacteria were highly attenuated in virulence and reverted to a phage-sensitive wild type in the absence of the selective pressure (36, 41, 44). Erskine (18) also observed delayed symptom development when pear slices were infected with a phage-resistant variant of *E. amylovora* which was not lysogenic. Therefore, the survival of insensitive host cells might not have a negative impact on the efficacy of phage application *in planta*.

Phage challenge and infection experiments demonstrated that selected two-phage cocktails can feature a much enhanced control efficacy on the growth of *E. amylovora*. Enhanced efficacy through the combined action of different types of phages with complementary host ranges represents a useful strategy and has been suggested for *E. amylovora* (49). Synergism of two or more different phages applied as a cocktail is likely based upon recognition of two different phage receptor molecules at the host cell surface and employment of different mechanisms for initial host cell takeover and virus multiplication. The exact reason for the apparently synergistic killing effect observed in our work is currently being investigated; preliminary data indicate a role of enzymes involved in depolymerizing the bacterial capsular material.

In conclusion, the results presented in this study demonstrate that the phages L1, M7, S6, and Y2 offer potential for phage-based biocontrol of fire blight. All four phages feature broad host ranges and virulent lifestyles. Detailed sequence analyses provided information to circumvent undesired transfer of host genetic material and facilitated selection of complementary phages for pooled applications.

ACKNOWLEDGMENTS

We thank Antonet Svircev for providing phage RFLP patterns, Jochen Klumpp for help with genome end analysis, Silvio Peng and Martin Zgraggen for assistance with phage isolation and characterization, and Jenna Denyes for helpful discussions.

This work was funded by the Swiss Federal Office for Agriculture (BLW Fire Blight Project—Biocontrol) and was conducted within the Swiss ProfiCrops and European Science Foundation COST Action 864 research networks.

REFERENCES

1. **Ackermann, H.-W.** 1996. Frequency of morphological phage descriptions in 1995. Arch. Virol. **141:**209–218.
2. **Adams, M. H.** 1959. Bacteriophages. Interscience Publishers Inc., New York, NY.
3. **Altschul, S. F., W. Gish, W. Miller, E. W. Myers, and D. J. Lipman.** 1990. Basic local alignment search tool. J. Mol. Biol. **215:**403–410.
4. **Balogh, B., B. I. Canteros, R. E. Stall, and J. B. Jones.** 2008. Control of citrus canker and citrus bacterial spot with bacteriophages. Plant Dis. **92:**1048–1052.
5. **Balogh, B., J. B. Jones, F. B. Iriarte, and M. T. Momol.** 2010. Phage therapy for plant disease control. Curr. Pharm. Biotechnol. **11:**48–57.
6. **Balogh, B., et al.** 2003. Improved efficacy of newly formulated bacteriophages for management of bacterial spot on tomato. Plant Dis. **87:**949–954.
7. **Billing, E.** 1960. An association between capsulation and phage sensitivity in *Erwinia amylovora*. Nature **186:**819–820.
8. **Bonn, W. G., and T. van der Zwet.** 2000. Distribution and economic importance of fire blight, p. 37–53. *In* J. L. Vanneste (ed.), Fire blight: the disease and its causative agent, *Erwinia amylovora.* CAB International, New York, NY.
9. **Casjens, S. R.** 2005. Comparative genomics and evolution of the tailed-bacteriophages. Curr. Opin. Microbiol. **8:**451–458.
10. **Casjens, S. R., and E. B. Gilcrease.** 2009. Determining DNA packaging strategy by analysis of the termini of the chromosomes in tailed-bacteriophage virions, p. 91–111. *In* M. R. J. Clokie and A. M. Kropinski (ed.), Bacteriophages: methods and protocols, vol. 2. Molecular and applied aspects. Humana Press, New York, NY.
11. **Casjens, S. R., et al.** 2005. The generalized transducing *Salmonella* bacteriophage ES18: complete genome sequence and DNA packaging strategy. J. Bacteriol. **187:**1091–1104.
12. **Ceyssens, P.-J., et al.** 2010. Molecular and physiological analysis of three *Pseudomonas aeruginosa* phages belonging to the "N4-like viruses." Virology **405:**26–30.
13. **Condron, B. G., J. F. Atkins, and R. F. Gesteland.** 1991. Frameshifting in gene 10 of bacteriophage T7. J. Bacteriol. **173:**6998–7003.

14. **Dobbins, A. T., et al.** 2004. Complete genomic sequence of the virulent *Salmonella* bacteriophage SP6. J. Bacteriol. **186:**1933–1944.
15. **Dorscht, J., et al.** 2009. Comparative genome analysis of *Listeria* bacteriophages reveals extensive mosaicism, programmed translational frameshifting, and a novel prophage insertion site. J. Bacteriol. **191:**7206–7215.
16. **Duffy, B., H.-J. Schärer, M. Bünter, A. Klay, and E. Holliger.** 2005. Regulatory measures against *Erwinia amylovora* in Switzerland. Bull. OEPP **35:** 239–244.
17. **Dunn, J. J., and F. W. Studier.** 1983. Complete nucleotide sequence of bacteriophage T7 DNA and the locations of T7 genetic elements. J. Mol. Biol. **166:**477–535.
18. **Erskine, J. M.** 1973. Characteristics of *Erwinia amylovora* bacteriophage and its possible role in the epidemiology of fire blight. Can. J. Microbiol. **19:**837–845.
19. **Falco, S. C., K. Vander Laan, and L. B. Rothman-Denes.** 1977. Virion-associated RNA polymerase required for bacteriophage N4 development. Proc. Natl. Acad. Sci. U. S. A. **74:**520–523.
20. **Flaherty, J. E., J. B. Jones, B. K. Harbaugh, G. C. Somodi, and L. E. Jackson.** 2000. Control of bacterial spot on tomato in the greenhouse and field with h-mutant bacteriophages. HortScience **35:**882–884.
21. **Gill, J. J., A. M. Svircev, R. Smith, and A. J. Castle.** 2003. Bacteriophages of *Erwinia amylovora*. Appl. Environ. Microbiol. **69:**2133–2138.
22. **Hagens, S., and M. J. Loessner.** 2010. Bacteriophage for biocontrol of foodborne pathogens: calculations and considerations. Curr. Pharm. Biotechnol. **11:**58–68.
23. **Hartung, J. S., D. W. Fulbright, and E. J. Klos.** 1988. Cloning of a bacteriophage polysaccharide depolymerase gene and its expression in *Erwinia amylovora*. Mol. Plant Microbe Interact. **1:**87–93.
24. **Hatfull, G. F.** 2008. Bacteriophage genomics. Curr. Opin. Microbiol. **11:**447–453.
25. **Jamalludeen, N., et al.** 2008. Complete genomic sequence of bacteriophage ΦEcoM-GJ1, a novel phage that has myovirus morphology and a podovirus-like RNA polymerase. Appl. Environ. Microbiol. **74:**516–525.
26. **Johnson, K. B., and V. O. Stockwell.** 2000. Biological control of fire blight, p. 319–337. *In* J. L. Vanneste (ed.), Fire blight: the disease and its causative agent, *Erwinia amylovora.* CAB International, New York, NY.
27. **Johnson, K. B., and V. O. Stockwell.** 1998. Management of fire blight: a case study in microbial ecology. Annu. Rev. Phytopathol. **36:**227–248.
28. **Jones, A. L., and E. L. Schnabel.** 2000. The development of streptomycin-resistant strains of *Erwinia amylovora*, p. 235–251. *In* J. L. Vanneste (ed.), Fire blight: the disease and its causative agent, *Erwinia amylovora.* CAB International, New York, NY.
29. **Kazmierczak, K. M., and L. B. Rothman-Denes.** 2006. Bacteriophage N4, p. 302–314. *In* R. Calendar (ed.), The bacteriophages, 2nd ed. Oxford University Press, New York, NY.
30. **Kilcher, S., M. J. Loessner, and J. Klumpp.** 2010. *Brochothrix thermosphacta* bacteriophages feature heterogeneous and highly mosaic genomes and utilize unique prophage insertion sites. J. Bacteriol. **192:**5441–5453.
31. **Kim, W.-S., and K. Geider.** 2000. Characterization of a viral EPS-depolymerase, a potential tool for control of fire blight. Phytopathology **90:**1263–1268.
32. **Klumpp, J., et al.** 2008. The terminally redundant, nonpermuted genome of *Listeria* bacteriophage A511: a model for the SPO1-like myoviruses of Gram-positive bacteria. J. Bacteriol. **190:**5753–5765.
33. **Kropinski, A. M., D. Prangishvili, and R. Lavigne.** 2009. Position paper: the creation of a rational scheme for the nomenclature of viruses of *Bacteria* and *Archaea*. Environ. Microbiol. **11:**2775–2777.
34. **Lehman, S. M.** 2007. Ph.D. thesis. Development of a bacteriophage-based biopesticide for fire blight. Brock University, St. Catharines, Ontario, Canada.
35. **Lehman, S. M., A. M. Kropinski, A. J. Castle, and A. M. Svircev.** 2009. Complete genome of the broad-host-range *Erwinia amylovora* phage ΦEa21-4 and its relationship to *Salmonella* phage Felix O1. Appl. Environ. Microbiol. **75:**2139–2147.
36. **Loc Carrillo, C., et al.** 2005. Bacteriophage therapy to reduce *Campylobacter jejuni* colonization of broiler chickens. Appl. Environ. Microbiol. **71:**6554–6563.
37. **Loessner, M. J., R. B. Inman, P. Lauer, and R. Calendar.** 2000. Complete nucleotide sequence, molecular analysis and genome structure of bacteriophage A118 of *Listeria monocytogenes*: implications for phage evolution. Mol. Microbiol. **35:**324–340.
38. **Molineux, I. J.** 2006. The T7 group, p. 277–301. *In* R. Calendar (ed.), The bacteriophages, 2nd ed. Oxford University Press, New York, NY.
39. **Momol, M. T., and H. S. Aldwinckle.** 2000. Genetic diversity and host range of *Erwinia amylovora*, p. 55–72. *In* J. L. Vanneste (ed.), Fire blight: the disease and its causative agent, *Erwinia amylovora.* CAB International, New York, NY.
40. **Müller, I., M. Kube, R. Reinhardt, W. Jelkmann, and K. Geider.** 2011. Complete genome sequences of three *Erwinia amylovora* phages isolated in North America and a bacteriophage induced from an *Erwinia tasmaniensis* strain. J. Bacteriol. **193:**795–796.
41. **O'Flynn, G., R. P. Ross, G. F. Fitzgerald, and A. Coffey.** 2004. Evaluation of a cocktail of three bacteriophages for biocontrol of *Escherichia coli* O157:H7. Appl. Environ. Microbiol. **70:**3417–3424.
42. **Ohmori, H., L. L. Haynes, and L. B. Rothman-Denes.** 1988. Structure of the ends of the coliphage N4 genome. J. Mol. Biol. **202:**1–10.
43. **Pajunen, M. I., M. R. Elizondo, M. Skurnik, J. Kieleczawa, and I. J. Molineux.** 2002. Complete nucleotide sequence and likely recombinatorial origin of bacteriophage T3. J. Mol. Biol. **319:**1115–1132.
44. **Randhawa, P. S., and E. L. Civerolo.** 1986. Interaction of *Xanthomonas campestris* pv. pruni with pruniphage and epiphytic bacteria on detached peach leaves. Phytopathology **76:**549–553.
45. **Ravensdale, M., T. J. Blom, J. A. Gracia-Garza, A. M. Svircev, and R. J. Smith.** 2007. Bacteriophages and the control of *Erwinia carotovora* subsp. *carotovora.* Can. J. Plant Pathol. **29:**121–130.
46. **Rezzonico, F., V. O. Stockwell, and B. Duffy.** 2009. Plant agricultural streptomycin formulations do not carry antibiotic resistance genes. Antimicrob. Agents Chemother. **53:**3173–3177.
47. **Ritchie, D. F., and E. J. Klos.** 1979. Some properties of *Erwinia amylovora* bacteriophages. Phytopathology **69:**1078–1083.
48. **Sambrook, J., and D. W. Russell.** 2001. Molecular cloning, 3rd ed., vol. 1. Cold Spring Harbor Laboratory Press, Cold Spring Harbor, NY.
49. **Schnabel, E. L., W. G. D. Fernando, M. P. Meyer, A. L. Jones, and L. E. Jackson.** 1999. Bacteriophage of *Erwinia amylovora* and their potential for biocontrol, p. 649–653. *In* M. T. Momol and H. Saygili (ed.), Proceedings of the 8th international workshop on fire blight, vol. 489. ISHS Acta Hortic., Leuven, Belgium.
50. **Schnabel, E. L., and A. L. Jones.** 2001. Isolation and characterization of five *Erwinia amylovora* bacteriophages and assessment of phage resistance in strains of *Erwinia amylovora*. Appl. Environ. Microbiol. **67:**59–64.
51. **Shine, J., and L. Dalgarno.** 1974. The 3′-terminal sequence of *Escherichia coli* 16S rRNA: complementarity to nonsense triplets and ribosome binding sites. Proc. Natl. Acad. Sci. U. S. A. **71:**1342–1346.
52. **Steven, A. C., et al.** 1988. Molecular substructure of a viral receptor-recognition protein—the gp17 tail-fiber of bacteriophage T7. J. Mol. Biol. **200:** 351–365.
53. **Stonier, T., J. McSharry, and T. Speitel.** 1967. *Agrobacterium tumefaciens* Conn IV. Bacteriophage $PB2_1$ and its inhibitory effect on tumor induction. J. Virol. **1:**268–273.
54. **Stummeyer, K., et al.** 2006. Evolution of bacteriophages infecting encapsulated bacteria: lessons from *Escherichia coli* K1-specific phages. Mol. Microbiol. **60:**1123–1135.
55. **Thierauf, A., G. Perez, and S. Maloy.** 2009. Generalized transduction, p. 267–286. *In* M. R. J. Clokie and A. M. Kropinski (ed.), Bacteriophages: methods and protocols, vol. 1: isolation, characterization, and interactions. Humana Press, New York, NY.
56. **Thomson, S. V.** 2000. Epidemiology of fire blight, p. 9–36. *In* J. L. Vanneste (ed.), Fire blight: the disease and its causative agent, *Erwinia amylovora.* CAB International, New York, NY.
57. **Vandenbergh, P. A., A. M. Wright, and A. K. Vidaver.** 1985. Partial purification and characterization of a polysaccharide depolymerase associated with phage-infected *Erwinia amylovora*. Appl. Environ. Microbiol. **49:**994–996.
58. **Vanneste, J. L., and S. Eden-Green.** 2000. Migration of *Erwinia amylovora* in host plant tissues, p. 73–83. *In* J. L. Vanneste (ed.), Fire blight: the disease and its causative agent, *Erwinia amylovora.* CAB International, New York, NY.
59. **Whichard, J. M., et al.** 2010. Complete genomic sequence of bacteriophage Felix O1. Viruses **2:**710–730.
60. **Wrigley, N. G.** 1968. Lattice spacing of crystalline catalase as an internal standard of length in electron microscopy. J. Ultrastruct. Res. **24:**454–464.
61. **Zhao, Y., K. Wang, N. Jiao, and F. Chen.** 2009. Genome sequences of two novel phages infecting marine roseobacters. Environ. Microbiol. **11:**2055–2064.
62. **Zimmer, M., E. Sattelberger, R. B. Inman, R. Calendar, and M. J. Loessner.** 2003. Genome and proteome of *Listeria monocytogenes* phage PSA: an unusual case for programmed +1 translational frameshifting in structural protein synthesis. Mol. Microbiol. **50:**303–317.